

Analytical calculation of sheet curvature in four-roll mills at tubes production

V. N. Shinkin, Dr. Phys.-Math., Professor¹, e-mail: shinkin-korolev@yandex.ru

¹National University of Science and Technology "MISiS" (Moscow, Russia)

Stationary bending of sheet metal on the electromechanical rolling mills demonstrates high productivity and efficiency, relevant for any modern enterprise. Regardless of the number of shafts, the operating principle of the mills is not complicated. The sheet blank is installed in the gap between the shafts, which rotate in different directions. Passing between the cylinders, the sheet bends and takes the desired shape. The main assortment of finished products, produced with the help of rollers, are details in the form of a cylinder, cone or oval. The cold bending method, which is the basis of the working process, does not destroy the metal and does not have a negative influence on its structure, as it sometimes happens during prolonged thermal exposure on metal alloys. The popularity of roller mills is largely due to their relatively low cost, as well as minimal outlay on maintenance and exploitation. If the company needs a cheaper and more economical mills, it is worth paying attention to manual models. For larger companies, the four-roller mills equipped with CNC-systems and operating in automatic regime are recommended. Modern models, produced by leading manufacturers, are favorably distinguished by visibility and ease of exploitation, attractive design, guaranteed safety and reliability. Such equipment is in demand in mass production, where high productivity and trouble-free operation of mills are appreciated. It is impossible to guess the sheet blank curvature in rolling new type of tube. This paper is devoted to the solution of this important problem and to analytical calculation of blank curvature in the four-roller mills.

Key words: curvature, four-roll mills, bend, tube, analytical calculation, mathematical modelling.

DOI: 10.17580/cisir.2022.01.10

Introduction

Depending on the tubes purpose, characteristics and dimensions of the source material, the welded tubes are obtained in several ways, each of which has its own technological advantages and disadvantages. The production methods of welded tubes can be classified according to two main distinctive features – according to the temperature of forming metal: cold sheet forming (all types of modern tube-electric welding units) and hot sheet forming (units of continuous furnace tube welding); according to the method of obtaining the final dimensions of finished tubes: obtaining the final dimensions of finished tubes on the calibration stands of molding-welding units; obtaining a limited number of sizes of tube blanks on tube-welding units and the final formation of the diameter and wall thickness on the hot or cold reduction mills.

Methods of production of welded tubes are also classified according to the process nature (continuous or discrete process), according to the number and direction of seams on tube (single seam, double seam, straight seam or spiral seam), according to the method of sheet forming into a tube billet (roll, press or semi-rolling type), according to the method of welding (furnace welding, arc welding under a layer of flux, electric resistance welding, induction welding, welding with high frequency currents, electric welding in an environment of inert gases, electron beam welding of tubes, direct current welding, plasma and ultrasonic welding) and the number of metal layers in the tube (single-layer, double-layer or multi-layer).

Depending on the technical requirements for the tubes, their assortment, the possibilities of obtaining the initial billet and the required productivity of the units, one or another method of welding and forming the billet is used, the most appropriate nature of the process and the design of the manufactured tubes are chosen. Forming (folding) of a flat tube billet (sheet, tape, strip) into a cylindrical one is one of the main operations of all technological processes for the production of welded tubes. The forming process requires significantly lower energy costs than rolling, which has a decisive influence on the technical and economic indicators of the welded tubes production.

The forming of the tube billet can be carried out at normal temperature (cold forming) and with preheating of the metal (hot forming). Hot forming of the tube billet is used at the continuous furnace welding of tubes and is carried out in driving rolls. As a result of the high plasticity of the heated metal, forming is possible in two pairs of rolls with a short length of the forming zone. In modern aggregates for the production of welded tubes, various cold forming methods are used: bending in mills, bending on presses, spiral forming and forming on continuous rolling mills. Forming in mills and on presses is used in the production of large-diameter tubes from sheets by arc welding under a layer of flux.

Under bending in mills, the sheet bends between the three or four rolls (Fig. 1). In three-roll mills [1], the diameter of the upper roll is larger than the diameter of the lower rolls. During the forming process, the rolls make a reversible movement, at that the upper (or the lower roll)

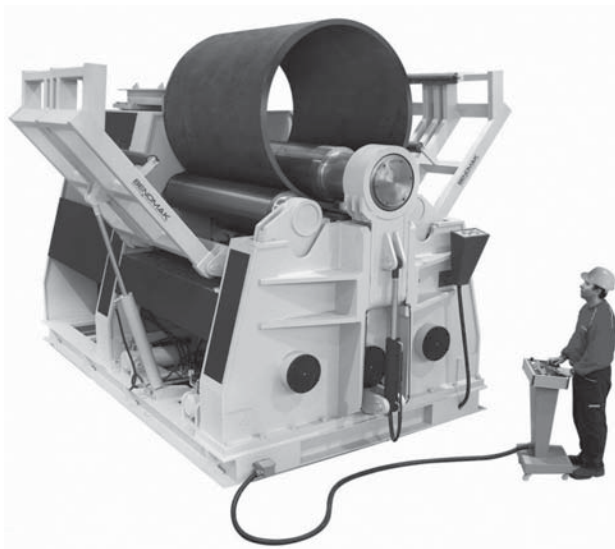


Fig. 1. Four-roller mills with hydraulic drive “Bendmak CY4R-HS 390-25/30”

can rise and descent to adjust the forming billet diameter. At this method of forming, the end extreme sections of the sheet, equal to half the distance between the lower side rolls, are obtained flat. This disadvantage is eliminated by pre-bending the sheet ends on the press or on the rolling mill. Besides that, at forming in rolling mills, the length of the obtained tubes is limited (no more than 6–8 m).

A more modern method of forming large-diameter straight-seam tubes is forming on presses, which can be made both with one cylindrical blank with pre-bending edges on a rolling mill and with two semi-cylindrical blanks at tubes welding from two sheets. In the production of spiral-seam tubes, a sheet of the same width is used for the manufacture of tubes of various diameters. The tube billet is formed by plastic bending of the strip in a plane located at some angle to the longitudinal axis of the sheet. The forming process of tube billet in the mills, press dies and continuous rolling rollers is considered as a process of plastic bending of strip with gradually increasing curvature. Under analyzing the stress-strain state of the metal during bending, the following assumptions are made: the cross-sections of the sheet remain flat and perpendicular to the longitudinal axis after deformation, and the thickness of the sheet does not change during plastic bending.

The purpose of this investigation is the new exact analytical calculation of steel sheet curvature at during shaping and after shaping on the four-roll mills, based on taking into account the exact analytical curve of steel hardening, depending on the Young's modulus, strength modulus, yield strength and ultimate strength of steel. Knowledge of sheet curvature sharply reduces the amount of spoilage at the output, significantly saves metal consumption, time and money, contributes to the formation of the optimal strategy for tube billet rolling.

Analytical calculation of dimensionless bending moment of sheet

The main mechanical characteristics of sheet steel are the young modulus E , the yield strength σ_y , the ultimate strength σ_u , the modulus hardening P_y in the yield strength, the relative elongation ε_y in the yield strength, the relative elongation ε_u in the ultimate strength (at the moment of neck formation) [2–4].

The main factor at shaping the tube billet, which answers for the curvature radius of the billet during its bending and after its springing-back, is the bending moment M of the sheet cross-section [1, 5–7]. The more accurate the approximation of the sheet bending moment, the more accurately residual radii of curvature of the billet are calculated after its elastic-plastic shaping on the four-roll mills.

The main geometrical characteristics at the sheet shaping [8–10] are the thickness h , the width b , the curvature k of the longitudinal median (neutral) line and the curvature radius $\rho = 1/k$. At $\rho \geq \rho_y = Eh/(2\sigma_y)$ is observed the purely elastic bending the flat sheet, and at $\rho < \rho_y = Eh/(2\sigma_y)$ is observed the elastoplastic bending the flat sheet [1, 11, 12].

The dimensionless bending moment in the sheet cross-section, corresponding to the direct cubic approximation of the steel hardening zone, has the form

$$F(Shi) = \frac{12M}{bh^2\sigma_y}, \quad Shi = \frac{Eh}{\sigma_y\rho}, \quad Shi(\rho_y) = 2, \quad \rho = \frac{Eh}{\sigma_y Shi},$$

$$F(Shi) = (Shi, \quad 0 \leq Shi \leq 2; \quad F_{plastic}(Shi), \quad Shi > 2), \quad (1)$$

$$\begin{aligned} F_{plastic}(Shi) = 3 - \frac{4}{Shi^2} + \frac{P_y}{E} Shi \left(1 - \frac{2}{Shi}\right)^2 \left(1 + \frac{1}{Shi}\right) - \\ - \frac{(2P_y(\varepsilon_u - \varepsilon_y) - 3(\sigma_u - \sigma_y)\sigma_y)}{4E^2(\varepsilon_u - \varepsilon_y)^2} Shi^2 \left(1 - \frac{2}{Shi}\right)^3 \left(\frac{3}{2} + \frac{1}{Shi}\right) + \\ + \frac{3\sigma_y^2(P_y(\varepsilon_u - \varepsilon_y) - 2(\sigma_u - \sigma_y))}{40E^3(\varepsilon_u - \varepsilon_y)^3} Shi^3 \left(1 - \frac{2}{Shi}\right)^4 \left(2 + \frac{1}{Shi}\right), \quad (2) \end{aligned}$$

where Shi is the dimensionless curvature of the longitudinal median line of sheet.

Analytical calculation of springing coefficient of sheet

After elastic-plastic bending, the sheet partially springs back. The process of sheet springing after bending is described with help of Hencky theorem. According to the Hencky theorem, the value of the residual curvature after springing is equal to

$$Shi_{res} = (0, \quad 0 \leq Shi \leq 2; \quad Shi - F_{plastic}(Shi), \quad Shi > 2). \quad (3)$$

At that, the springing coefficient β_{res} , the residual curvature k_{res} and the curvature residual radius ρ_{res} of the sheet neutral line are respectively equal to

$$\beta(Shi) = \begin{cases} \infty, & 0 \leq Shi \leq 2; \\ \frac{Shi}{Shi - F_{plastic}(Shi)}, & Shi > 2 \end{cases} \quad (4)$$

$$k_{res} = \frac{1}{\beta} k = \begin{cases} 0, & 0 \leq Shi \leq 2; \\ \frac{Shi - F_{plastic}(Shi)}{Shi} k, & Shi > 2 \end{cases} \quad (5)$$

$$\rho_{res} = \beta \rho = \begin{cases} \infty, & 0 \leq Shi \leq 2; \\ \frac{Shi}{Shi - F_{plastic}(Shi)} \rho, & Shi > 2 \end{cases} \quad (6)$$

The bending scheme of sheet into tube billet on four-roll mills

There are a large number of different schemes for bending a thick-walled sheet into a round tube billet on the four-roll mills. Below, as a typical example, the rolling scheme of a sheet into a tube billet during three and a half oppositely directed (clockwise and counterclockwise) full turns of billet is shown (Fig. 2).

Feeding (loading) a sheet into the mills. In the beginning, the sheet is fed into the mills and clamped so that the longitudinal edges (end-faces) of the sheet and the axes of all four rolls of the mills are parallel (Fig. 2, a, b). For that, the axes of four shafts (of the upper shaft, the lower shaft, the right-side shaft and the left-side shaft) should be directed

parallel to each other. Next, the left-side roll is slightly raised up above the right-side roll (Fig. 2, a). Then, the sheet is fed by the roll-table over the right-side roll to the stop of the left longitudinal edge of the sheet in the left-side roll of the mills and the sheet is pressed tightly without a gap to the surface of the left-side roll (Fig. 2, a). At that, the longitudinal edge of the sheet becomes parallel to the axis of the left-side roll.

Clamping the sheet between the upper and lower rolls. Next, the lower roll is risen up and rigidly clamps the sheet between the upper and lower rolls (Fig. 2, b). Then, the right roll is risen up, touches the sheet and supports the left part of the sheet in a horizontal position (Fig. 2, b). Then, the left-side roll goes down and loses contact with the sheet (Fig. 2, b). Then, the sheet is slightly fed to the right by means of rotating the upper roll so that the left edge of the sheet protrudes minimally to the left from the clamping point of the sheet between the upper and lower rolls (Fig. 2, b).

Bending and rolling of the sheet in a clockwise direction (the first full turn of the upper roll). Next, the right-side roll is risen up by the amount of sheet compression $H_1 > 0$, bending the left part of the sheet up (Fig. 2, c). Then, the sheet is rolling clockwise between the upper roll, the lower roll and the right-side roll (Fig. 2, d) until the right edge of the sheet touches the surface of the right-side roll (Fig. 2, e).

Bending and rolling of the sheet counterclockwise (the second full turn of the upper roll). Next, the left-side roll is risen up by the amount of sheet compression $H_2 \geq H_1$, bending the right part of the sheet up, and the right-side roll lowers down and loses contact with the sheet (Fig. 2, f). Then, the sheet is rolling slightly clockwise so that the right edge of the sheet protrudes minimally to the right of the sheet clamping point between the upper and lower rolls (Fig. 2, g). Next, the sheet is rolling counterclockwise between the upper roll, the lower roll and the left-side roll (Fig. 2, h) until the sheet left edge touches the surface of the left-side roll (Fig. 2, i).

Bending and rolling of the sheet in a clockwise direction (the third full turn of the upper roll). Then, the right-side roll is risen up by the amount of sheet compression $H_3 \geq H_2$, bending the right part of the sheet up, and the left-side roll lowers down and loses contact with the sheet (Fig. 2, j). Next, the sheet is rolling slightly counterclockwise so that the sheet left edge protrudes minimally to the left from the clamping point of the sheet between the upper and lower rolls (Fig. 2, k). Then, the sheet is rolled clockwise between the upper roll, the lower roll and the right-side roll (Fig. 2, l) until the sheet right edge touches the surface of the right-side roll (Fig. 2, m).

Bending and rolling of the sheet counterclockwise (half-turn of the upper roll). Next, the left-side roll is risen up by the amount of sheet compression $H_4 \geq H_3$, bending the right part of the sheet up, and the right-side roll lowers down and loses contact with the sheet (Fig. 2, n). Then, the sheet is rolling slightly clockwise so that the sheet right

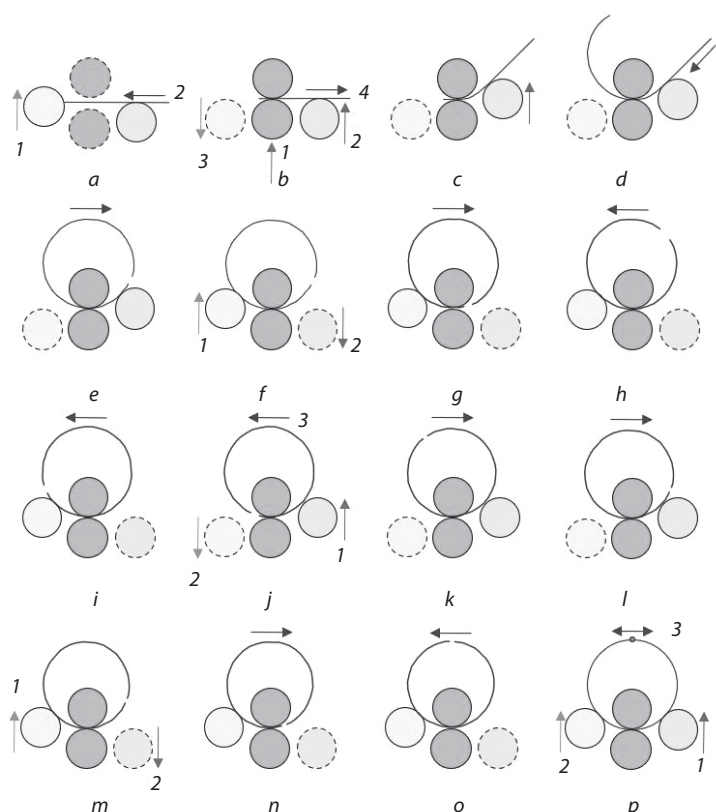


Fig. 2. The bending scheme of sheet on four-roll mills

edge protrudes minimally to the right of the clamping point of the sheet between the upper and lower rolls (Fig. 2, *n*). Next, the sheet is rolled counterclockwise for a half-turn so that the right and left edges of the sheet are raised up as high as possible and are symmetrically positioned relative to the vertical line passing through the centers of the cross-sections of the upper and lower rolls (Fig. 2, *o*).

Finishing bending the tube billet until the junction of sheet edges. Then, the left and right-side rolls are simultaneously lifted up by the same amount of sheet compression $H_5 \geq H_4$, bending the left and right parts of the sheet up so that the left and right edges of the sheet touch (Fig. 2, *p*). Next, the sheet is rolled between the upper roll, the lower roll, the left-side roll and the right-side roll clockwise and counterclockwise until an ideal uniform roundness of the cross-section of the tube billet is obtained (Fig. 2, *p*).

Removing the tube billet from the mills. After the final rolling, the lower roll descends down and loses contact with the sheet, and the joining point of the sheet edges is rotated as down as possible by means of rotating the upper roll. Then, the left and right-side rolls are simultaneously lowered down until the upper roll loses contact with the sheet. Next, the lock of the upper roll is removed by the special mechanism of the mills from one end of the upper roll, and the tube billet rises up and is removed by the special crane from the mills.

Assembly and welding the tube billet. Then, the tube billet is transported to the place of assembly and welding of the tube. Next, the assembly of the tube edges by the gas burner from the inside of the tube comes. Then, the three-, four- or five-arc welding (in depending on the thickness of the tube) of the tube edges takes place, first from the outside of the tube, and then from the inside of the tube. Then, the expansion operation of the tube on the expander is followed to obtain the most accurate tube diameter and an ideal uniform curvature of the tube wall.

Note that the shortened variants of the above-mentioned scheme of rolling a sheet into a tube billet can be used under rolling a sheet for one full turn of the upper roll (Fig. 2, *a–g*), for two full turns of the upper roll (Fig. 2, *a–j*) and for three full turns of the upper shaft (Fig. 2, *a–n*) without finishing bending the tube billet until the billet edges' contact (Fig. 2, *o, j*).

Analytical calculation of sheet curvature at its shaping in four-roll mills

The sheet curvature at the first turn of the upper roll clockwise (Fig. 3, Fig. 2, *d*). Let h be the thickness of the sheet; r_{10} and r_{20} be the radii of the right and left-side rolls ($r_1 = r_{10} + h/2$, $r_2 = r_{20} + h/2$); φ_1 be the contact angle of the right-side roll with the sheet (the point *A*); k_1 and $\rho_1 = 1/k_1$ be the curvature and curvature radius of the sheet middle line at the point of clamping the sheet (on the right of the point *O*) between the upper and lower rolls; H_{10} be the sheet compression by the right-side roll ($H_1 = H_{10} + h$); t_1 and z_1

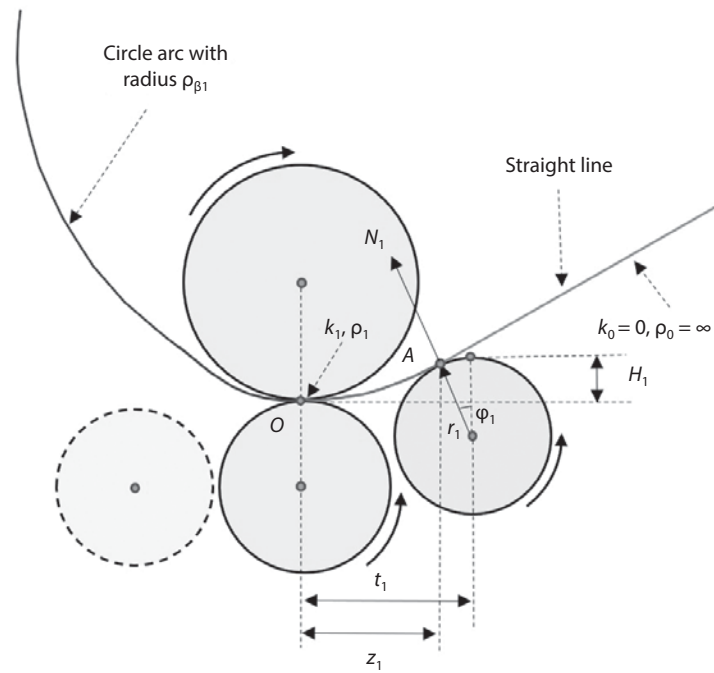


Fig. 3. Calculation scheme at the first turn of the upper roll clockwise

be the coordinates of the center of the right-side roll and the point *A* (Fig. 3).

The angle φ_1 is found from the nonlinear equation

$$4\operatorname{tg} \varphi_1(t_1 - r_1 \sin \varphi_1) = 6H_1 - 6r_1(1 - \cos \varphi_1). \quad (7)$$

Next, we find the curvature radius ρ_1 and the curvature k_1 of the sheet middle line at the point of clamping the sheet (on the right) between the upper and lower rolls:

$$\rho_1 = \frac{t_1 - r_1 \sin \varphi_1}{2\operatorname{tg} \varphi_1}, \quad k_1 = \frac{1}{\rho_1}, \quad z_1 = t_1 - r_1 \sin \varphi_1. \quad (8)$$

The support reaction at the point of sheet contact (the point *A*) with the right-side roll is equal to

$$N_1 = \frac{bh^2\sigma_y}{12(t_1 \cos \varphi_1 - (r_1 - H_1) \sin \varphi_1)} fN_1, \quad (9)$$

$$fN_1 = 3 - 4 \left(\frac{\sigma_y \rho_1}{Eh} \right)^2 + 2 \frac{P_y}{\sigma_y} \left(\frac{h}{2\rho_1} \right) \left(1 - 2 \frac{\sigma_y \rho_1}{Eh} \right)^2 \left(1 + \frac{\sigma_y \rho_1}{Eh} \right) -$$

$$- \frac{2P_y(\varepsilon_u - \varepsilon_y) - 3(\sigma_u - \sigma_y)}{\sigma_y (\varepsilon_u - \varepsilon_y)^2} \left(\frac{h}{2\rho_1} \right)^2.$$

$$\cdot \left(1 - 2 \frac{\sigma_y \rho_1}{Eh} \right)^3 \left(\frac{3}{2} + \frac{\sigma_y \rho_1}{Eh} \right) + \frac{3}{5} \frac{P_y(\varepsilon_u - \varepsilon_y) - 2(\sigma_u - \sigma_y)}{\sigma_y (\varepsilon_u - \varepsilon_y)^3} \cdot \left(\frac{h}{2\rho_1} \right)^3 \left(1 - 2 \frac{\sigma_y \rho_1}{Eh} \right)^4 \left(2 + \frac{\sigma_y \rho_1}{Eh} \right).$$

To the left of the clamping point of the sheet (the point *O*) between the upper and lower rolls, the sheet springs partially

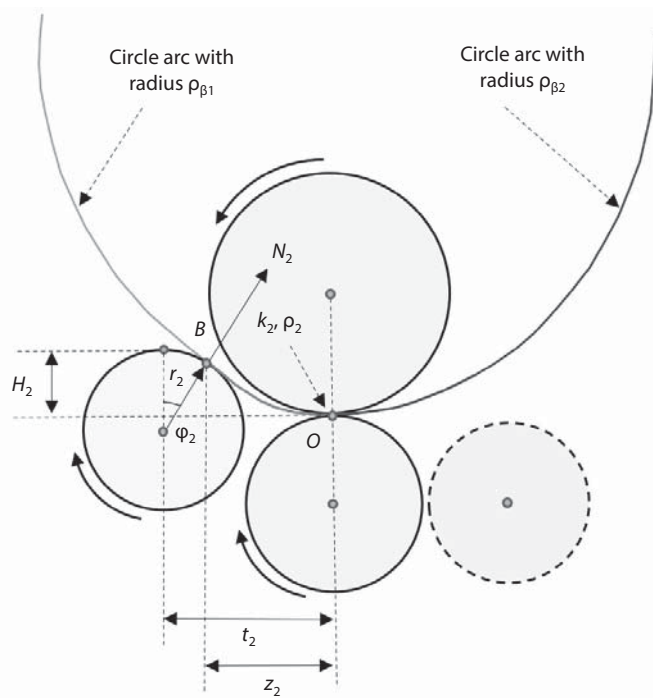


Fig. 4. Calculation scheme at the second turn of the upper roll counter-clockwise

back, and the curvature radius of the middle line of the sheet is equal to $\rho_{\beta 1} = \beta(Eh/\sigma_y\rho_1)\rho_1$, $k_{\beta 1} = 1/\rho_{\beta 1}$.

The tube billet curvature at the second turn of the upper roll counter-clockwise (Fig. 4, Fig. 2, h). Let φ_2 be the contact angle of the left-side roll with the sheet (the point B); k_2 and $\rho_2 = 1/k_2$ be the curvature and curvature radius of the sheet middle line at the point of clamping the sheet (on the left of the point O) between the upper and lower rolls; H_2 be the sheet compression by the left-side roll ($H_2 = H_{20} + h$); t_2 and z_2 be the coordinates of the center of the left-side roll and the point B (Fig. 4).

The angle φ_2 is found from the nonlinear equation

$$\begin{aligned} & \left(4\tg\varphi_2 - k_{\beta 1}(t_2 - r_2 \sin\varphi_2)\right)\left(1 + \tg^2\varphi_2\right)^{3/2}\left(t_2 - r_2 \sin\varphi_2\right) = \\ & = 6H_2 - 6r_2(1 - \cos\varphi_2). \end{aligned} \quad (10)$$

Next, we find the curvature radius ρ_2 and curvature k_2 of the sheet middle line at the point of clamping the sheet (on the left) between the upper and lower rolls:

$$\begin{aligned} \rho_2 &= \frac{t_2 - r_2 \sin\varphi_2}{2\tg\varphi_2 - k_{\beta 1}(t_2 - r_2 \sin\varphi_2)\left(1 + \tg^2\varphi_2\right)^{3/2}}, \\ k_2 &= \frac{1}{\rho_2}, \quad z_2 = t_2 - r_2 \sin\varphi_2. \end{aligned} \quad (11)$$

The support reaction at the point of sheet contact (the point B) with the left-side roll is equal to

$$N_2 = \frac{bh^2\sigma_y}{12(t_2 \cos\varphi_2 - (r_2 - H_2) \sin\varphi_2)} fN_2, \quad (12)$$

$$\begin{aligned} fN_2 &= 3 - 4\left(\frac{\sigma_y\rho_2}{Eh}\right)^2 + 2\frac{P_y}{\sigma_y}\left(\frac{h}{2\rho_2}\right)\left(1 - 2\frac{\sigma_y\rho_2}{Eh}\right)^2 \\ &\cdot \left(1 + \frac{\sigma_y\rho_2}{Eh}\right) - \frac{2P_y(\varepsilon_u - \varepsilon_y) - 3(\sigma_u - \sigma_y)\left(\frac{h}{2\rho_2}\right)^2}{\sigma_y(\varepsilon_u - \varepsilon_y)^2} \\ &\cdot \left(1 - 2\frac{\sigma_y\rho_2}{Eh}\right)^3 \left(\frac{3}{2} + \frac{\sigma_y\rho_2}{Eh}\right) + \frac{3}{5} \frac{P_y(\varepsilon_u - \varepsilon_y) - 2(\sigma_u - \sigma_y)}{\sigma_y(\varepsilon_u - \varepsilon_y)^3} \\ &\cdot \left(\frac{h}{2\rho_2}\right)^3 \left(1 - 2\frac{\sigma_y\rho_2}{Eh}\right)^4 \left(2 + \frac{\sigma_y\rho_2}{Eh}\right). \end{aligned}$$

To the right of the clamping point of the sheet (the point O) between the upper and lower rolls, the sheet springs partially back, and the curvature radius of the middle line of the sheet is equal to $\rho_{\beta 2} = \beta(Eh/\sigma_y\rho_2)\rho_2$, $k_{\beta 2} = 1/\rho_{\beta 2}$.

Similarly, it is possible to find the curvature and curvature radius of the tube billet at the third turn of the upper roll clockwise (Fig. 2, k) and at the final half-turn of the upper roll counter-clockwise (Fig. 2, o).

Conclusions

The paper describes in detail the rolling (bending) processes of steel sheet on the four-roll mills in the production of the large diameter tubes. New dependences are obtained for the bending moment during sheet shaping, depending on the steel mechanical characteristics and the sheet geometrical characteristics (the thickness, the width, the curvature radius), with which new expressions are obtained for the curvature radius of the sheet at its bending on the four-roll mills. The new expression for the spring-back coefficient of sheet after its rolling has also been obtained, which allows calculating the curvature radius of sheet after its springing. The new obtained results will help the tube technologists at the metallurgical plants to reduce the amount of spoilage at the output, to save the metal consumption, to lower the production costs and to develop analytically the optimal strategy for rolling the tube billets on the four-roll mills. The obtained results can be successfully applied at the Vyksa Steel Works, Chelyabinsk Tube Rolling Plant, Izhora Pipe Mill, Volzhsky Pipe Plant, Zagorsk Pipe Plant, Magnitogorsk Iron and Steel Works and Cherepovets Steel Mill in the production of the thick-walled single-seam steel pipes of large-diameter on mills.

as

REFERENCES

- Shinkin V. N. Calculation of parameters of the asymmetrical three-roller sheet-bending rolls in steel pipes production. *Izvestiya Ferrous Metallurgy*. 2017. Vol. 60, No. 4. pp. 285–291.
- Shinkin V. N. Influence of non-linearity of hardening curve on elasticplastic bend of rectangular rod. *CIS Iron and Steel Review*. 2019. Vol. 17. pp. 39–42.
- Belskiy S. M., Shopin I. I. Mathematical model of the probability of strip breakage during cold rolling. *Chernye Metally*. 2020. No. 3. pp. 18–23.

4. Song D.-L., Zhang Y.-C., Du J.-F., Yi X.-C., Sun Y.-B., Cui Y.-H. Deformation analysis and parameters optimization for tension-bending leveling of strip. *Journal of Plasticity Engineering*. 2021. Vol. 28. No. 10. pp. 84–90.
5. Fadeev V., Kondrushev A. Special aspects of determining parameters for continuous deformation of pipe billets for the specified pipes size range. *Materials Today: Proceedings*. 2021. Vol. 38. pp. 1322–1325.
6. Fedorov V. A., Ushakov I. V., Permyakova I. E. Mechanical properties and crystallization of an annealed cobalt-based amorphous alloy. *Russian Metallurgy (Metally)*. 2004. Vol. 2004. No. 3. pp. 293–297.
7. Wang W.-B. Stability analysis of cross-section of double-row large-diameter pipeline based on BIM technology. *International Journal of Industrial and Systems Engineering*. 2021. Vol. 39. No. 2. pp. 162–175.
8. Belskiy S. M., Shopin I. I., Safronov A. A. Improving efficiency of rolling production by predicting negative technological events. *Defect and Diffusion Forum*. 2021. Vol. 410. pp. 96–101.
9. Goncharuk A. V., Fadeev V. A., Kadach M. V. Seamless pipes manufacturing process improvement using mandreling. *Solid State Phenomena*. 2021. Vol. 316. pp. 402–407.
10. Li X. Theoretical analysis on structural mechanics for multi-roll straightener of plate. *Forging and Stamping Technology*. 2020. Vol. 45. No. 11. pp. 134–142.
11. Shinkin V. N. Simplified method for calculation of bending moments of steel sheet and reactions of working rollers in multiroll straightening machine. *Izvestiya Ferrous Metallurgy*. 2017. Vol. 60. No. 10. pp. 777–784.
12. Li S., Wei C., Long Y. Deformation Analysis of Engineering Reinforcement Straightening Based on Bauschinger Effect. *International Journal of Steel Structures*. 2020. Vol. 20. No. 1. pp. 1–12.